Heterotrophic Bacteria Exhibit a Wide Range of Rates of Extracellular Production and Decay of Hydrogen Peroxide

Robin J. Bond[1]*, Colleen M. Hansel[2] and Bettina M. Voelker[3]

[1] *The Evergreen State College, Olympia, WA, United States, [2] Department of Marine Chemistry and Geochemistry, Woods Hole Oceanographic Institution, Woods Hole, MA, United States, [3] Department of Chemistry and Geochemistry, Colorado School of Mines, Golden, CO, United States*

Bacteria have been implicated as both a source and sink of hydrogen peroxide (H_2O_2), a reactive oxygen species which can both impact microbial growth and participate in the geochemical cycling of trace metals and carbon in natural waters. In this study, simultaneous H_2O_2 production and decay by twelve species of heterotrophic bacteria were evaluated in both batch and flow-through incubations. While wide species-to-species variability of cell-normalized H_2O_2 decay rate coefficients [2×10^{-8} to 5×10^{-6} hr^{-1} (cell $mL^{-1})^{-1}$] was observed, these rate coefficients were relatively consistent for a given bacterial species. By contrast, observed production rates (below detection limit to 3×10^2 amol $cell^{-1}$ hr^{-1}) were more variable even for the same species. Variations based on incubation conditions in some bacterial strains suggest that external conditions may impact extracellular H_2O_2 levels either through increased extracellular production or leakage of intracellular H_2O_2. Comparison of H_2O_2 production rates to previously determined superoxide (O_2^-) production rates suggests that O_2^- and H_2O_2 production are not necessarily linked. Rates measured in this study indicate that bacteria could account for a majority of H_2O_2 decay observed in aqueous systems but likely only make a modest contribution to dark H_2O_2 production.

Keywords: reactive oxygen species, hydrogen peroxide, heterotrophic bacteria, H_2O_2 production, H_2O_2 decomposition

INTRODUCTION

Hydrogen peroxide (H_2O_2) is ubiquitous in natural water systems and contributes to the biogeochemical cycling of trace metals. H_2O_2 production in natural waters was previously thought to occur primarily through the dismutation of photochemically produced superoxide (O_2^-) (Cooper et al., 1988; Shaked et al., 2010) but in recent years it has been shown to occur under dark conditions (Vermilyea et al., 2010a and 2010b; Dixon et al., 2013; Marsico et al., 2015; Zhang et al., 2016a), indicating that other production pathways exists. Experiments comparing H_2O_2 production of filtered to that of unfiltered natural water samples (e.g., Moffett and Zafiriou, 1990; Vermilyea et al., 2010b; Marsico et al., 2015;

Zhang et al., 2016b) suggest that biological production may be a strong contributor to overall H_2O_2 concentrations in natural waters.

The specific contribution of bacteria to H_2O_2 production and how it varies at the species level remains untested. Culture studies on (extracellular) biological H_2O_2 production by marine biota have, to date, focused on phytoplankton such as raphidophytes (see Marshall et al., 2002), coccolithophores (Palenik et al., 1987), and diatoms (Milne et al., 2009; Waring et al., 2010; Schneider et al., 2016; Cho et al., 2017). However, several recent studies (Learman et al., 2011; Diaz et al., 2013; Zhang et al., 2016a; Hansel et al., 2018; Sutherland et al., 2019) have shown that heterotrophic bacteria may be a substantial source of extracellular O_2^-. While O_2^- is a possible precursor of H_2O_2, whether these organisms also produce extracellular H_2O_2 has not been directly explored. Since H_2O_2 production rates are not necessarily linked to those of O_2^- (Schneider et al., 2016; Zhang et al., 2016a), known O_2^- production rates do not allow for estimation of H_2O_2 production.

The competing processes of H_2O_2 production and decay occur simultaneously in natural water systems, and H_2O_2 decay has been strongly linked to biological processes. For instance, 0.2-mm filtration of seawater led to a substantial decrease in decay (Petasne and Zika, 1997; Yuan and Shiller, 2001). Within a freshwater system, small algae (1–12 mm) and bacteria (0.2–1 mm) were found to be responsible for the majority of H_2O_2 decay (Cooper et al., 1994). Culture studies showed that increasing concentrations of heterotrophic bacteria *Vibrio pelagius* (Petasne and Zika, 1997), *Vibrio alginolyticus*, and *Enterobacter cloacae* (Cooper et al., 1994) increased decay rates, and that the presence of cyanobacterium *Synechococcus* – rather than secreted enzymes from that organism – was responsible for increased decay in seawater (Petasne and Zika, 1997). Morris et al. (2016) showed that, in seawater samples, many gene transcripts related to hydroperoxidase enzymes were linked to Alphaproteobacteria and Alteromonadales. Morris et al. (2011) has also shown that the abundant marine cyanobacterium *Prochlorococcus* lacks the ability to degrade H_2O_2 and instead relies on heterotrophic bacteria to lower H_2O_2 concentrations to non-toxic levels. Thus, bacterial degradation of H_2O_2 is likely to be an important control on H_2O_2 concentrations in many natural waters. However, the variability in the capacity and rates of H_2O_2 decay among heterotrophic bacteria is currently unknown.

Accordingly, the goal of this study was to compare rates of bacterial H_2O_2 production and decay across a wide range of species. Twelve species of common heterotrophic bacteria were chosen from among the organisms used by Diaz et al. (2013) to represent a wide phylogenetic diversity and variety of habitats (benthic vs. planktonic; estuarine vs. marine as well as one freshwater bacterium), as well as a wide range of measured extracellular superoxide production rates. Two different methods – a flow-through method similar to that used by Diaz et al. (2013) and a batch-style incubation better suited for evaluating systems with high decay rates – were used to determine H_2O_2 production rates and decay rate coefficients.

MATERIALS AND METHODS

Organisms: Growth and Experimental Conditions

All bacterial strains were obtained from the Hansel lab at Woods Hole Oceanographic Institution and are the same cultures used in Diaz et al., 2013 (**Table 1**). Cultures were inoculated from freezer stocks into the growth medium and incubated at 30°C until mid-exponential phase. An aliquot was then used to start experimental cultures, which were grown to mid-exponential phase, with growth tracked by measuring optical density at 600 nm, before being harvested for the experiment.

Growth and Experimental Conditions

Growth media were either LB medium (Sigma) made with 1 mM HEPES buffer (for *S. oneidensis* sp. MR-1) or, for all other cultures, a modified K medium (Andersened., 2005) made in 75% artificial seawater (van Waasbergen et al., 1993) as specified in Diaz et al. (2013). Once the cell reached exponential phase, cells were transferred into and analyzed within a minimal assay media to prevent H_2O_2 production from medium components. The assay media for H_2O_2 experiments were either deionized water (for *S. oneidensis* sp. MR-1) or, for the remaining cultures, 75% artificial seawater (NaCl, MgSO₄, CaCl₂, and KCl as specified in van Waasbergen et al., 1993) containing no additional nutrients.

Cell density of the cultures was determined by counting cells stained with DAPI (4′,6-diamidino-2-phenylindole) under an epifluorescent microscope, using an average count for ten fields of view. An estimated number for metabolically active cells was obtained by assuming the percentages of metabolically active cells were similar to those measured in Diaz et al. (2013) for the same species (49–97% for the twelve species examined in the present study).

H_2O_2 Detection

H_2O_2 was measured using the base-catalyzed chemiluminescent reaction with acridinium ester (AE) using a Waterville Analytical FeLume system as described by Cooper et al. (2000) and King et al. (2007). In summary, a slug of sample was pushed into the system by a carrier stream consisting of a catalase-treated (10 U mL⁻¹) solution of sterile assay medium (**Table 1**) and combined with acridinium ester reagent (5 mM, pH 3) in a mixing tee. Next, the sample/AE mixture combined with carbonate buffer (0.02 M, pH 10.6) in a flow cell. The photons produced by this reaction were then measured by a photomultiplier tube.

A calibration curve consisting of standard additions of H_2O_2 stock to aliquots of assay medium was implemented at the beginning of each experimental day.

Assessment of H_2O_2 Production Rates and Recovery Percentages With Flow-Through Methodology

H_2O_2 production and decay were quantified by measuring the effluent from cells immobilized on a filter, as in Milne et al. (2009) and modified to correct for breakdown of H_2O_2 by cells as described in Schneider et al. (2016).

TABLE 1 | Bacterial strains selected for present study.

Species	Habitat type/Strain source	Superoxide production	Growth medium	Assay medium
A. manganoxydans sp. SI85-9A1	Marine/planktonic; Coastal OR, United States	**	K	100% ASW
Bacillus sp. AzsLept-1c	Estuarine/benthic; Elkhorn Slough, CA, United States	****	K	75% ASW
Erythrobacter sp. SD-21	Marine/benthic; San Diego Bay, CA, United States	*	K	100% ASW
Halomonas sp. VMMm1-3c	Estuarine/benthic; Elkhorn Slough, CA, United States	**	K	75% ASW
Marinobacter sp. AzsJAc-4	Estuarine/benthic; Elkhorn Slough, CA, United States	***	K	75% ASW
Paracoccus sp. HIJAc-3c	Estuarine/planktonic; Elkhorn Slough, CA, United States	***	K	75% ASW
R. pomeroyi sp. DSS-3	Marine/planktonic; Coastal GA, United States	**	K	75% ASW
Shewanella sp. ANA-3	Estuarine/benthic; Woods Hole, MA, United States	**	K	75% ASW
S. oneidensis sp. MR-1	Freshwater/benthic; Lake Oneida, MA, United States	*	LB	DI water
Sulfitobacter sp. EE-36	Estuarine/planktonic; Coastal Georgia, United States	*	K	75% ASW
Tenacibaculum sp. UAzPsLept-5	Estuarine/benthic; Elkhorn Slough, CA, United States	*	K	75% ASW
Vibrio sp. A535	Marine/planktonic; BATS Station, Bermuda	***	K	75% ASW

Superoxide production is rated as follows: *below 0.5 amol cell^{-1} hr^{-1}; **0.5-2.0 amol cell^{-1} hr^{-1}; ***2.0–5.0 amol cell^{-1} hr^{-1}; ****above 5.0 amol cell^{-1} hr^{-1}. Except for S. oneidensis, assay media were full strength or diluted artificial seawater (ASW) from recipe found in van Waasbergen et al. (1993).

For each experimental run, the sterile assay medium indicated in **Table 1** flowed through a peristaltic pump at 0.6 mL min^{-1} over an empty acid-washed 25 mm 0.45-mm cellulose acetate syringe filter (VWR) and directly into the FeLume system until a constant concentration of H$_2$O$_2$ ([H$_2$O$_2$]$_{unspiked,direct}$) was detected, about 15 min. After 2.50 mL of culture was loaded onto the filter through the intake tube of the peristaltic pump, assay medium was flowed over the cells until a relatively stable signal was produced (about 10–15 min) and [H$_2$O$_2$] of the effluent ([H$_2$O$_2$]$_{unspiked,cells}$) was measured. Next, assay medium spiked with additional H$_2$O$_2$ was flowed over the cells until steady-state [H$_2$O$_2$] ([H$_2$O$_2$]$_{spiked,cells}$) could be measured. Finally, the filter was disconnected from the stream so that [H$_2$O$_2$] of the spiked medium ([H$_2$O$_2$]$_{spiked,direct}$) could be quantified.

Recovery (Rec$_{H2O2}$) for each experimental run was calculated with the equation:

$$Rec_{H2O2} = \frac{[H_2O_2]_{spiked,\ cells} - [H_2O_2]_{unspiked,\ cells}}{[H_2O_2]_{spiked,\ direct} - [H_2O_2]_{unspiked,\ direct}} \quad (1)$$

The denominator in eq. 1 represents the increase in [H$_2$O$_2$] in the medium due to the addition of the H$_2$O$_2$ spike, and the numerator represents the measured increase in the presence of cells. Calculation of recovery in this manner assumes that the cells on the filter break down the same fraction of H$_2$O$_2$ from both the spiked and the unspiked medium, i.e., that decay is first-order with respect to [H$_2$O$_2$].

The increase in [H$_2$O$_2$] due to the cells' production, [H$_2$O$_2$]$_{cell}$ (mol L^{-1}) and a cell-normalized production rate P$_{H2O2}$ (mol cell^{-1} hr^{-1}) were then calculated with the equations:

$$[H_2O_2]_{cell} = \frac{[H_2O_2]_{unspiked,\ cells}}{Rec_{H2O2}} - [H_2O_2]_{unspiked,\ direct} \quad (2)$$

and

$$P_{H2O2} = \frac{[H_2O_2]_{cell} \times Q}{N} \quad (3)$$

where Q is the flow rate (L hr^{-1}), and N is the number on the cells on the filter, calculated from the measured cell density in the experimental culture and the volume of culture loaded onto the filter.

Measurement of H$_2$O$_2$ Production and Decay Rates by Spiked Batch Incubations

The H$_2$O$_2$ production rate (P$_{H2O2}$) and the pseudo-first order decay coefficient (k$_{loss,H2O2}$) were determined by comparing the development of [H$_2$O$_2$] over time in batch incubations with different initial [H$_2$O$_2$]. This method is described by Vermilyea et al. (2010b), and will be referred to here as spiked batch incubations. The method was modified as follows to be used with cultures instead of field samples.

5.00 mL aliquots of bacterial culture were centrifuged at 1000 rpm for 10 min, the supernatant was removed, and the cells were resuspended in fresh assay medium indicated in **Table 1**. Previous experiments with these species and others closely related indicated that the supernatant is primarily cell-free and has similar reactivity (for instance, in terms of superoxide production and Mn(II) oxidation) to that obtained via filtration (0.2 mm) (e.g., Learman et al., 2011; Diaz et al., 2013). Resuspended cultures were combined with additional assay medium and, in some cases, spiked with 5.00 mM H$_2$O$_2$ stock, so that each incubation was performed on a total volume of 40.0 mL. Samples were incubated in sterile syringes (Kendell Mono-Ject 50 mL) with a magnetic stir bar to facilitate mixing. In previous experiments, syringes with rubber-lined plungers were found to contribute to [H$_2$O$_2$] decay after prolonged contact with seawater. The syringes used in these experiments had plastic plungers. Total H$_2$O$_2$ levels for each syringe were analyzed over a period of time necessary for [H$_2$O$_2$] to reach steady state (∼15 min to 2 h, depending on bacterial strain).

To model simultaneous production and decay, it was assumed that the production rate of H$_2$O$_2$ in the medium (mol L^{-1} h^{-1}), P$_{H2O2}$, was constant and that both P$'_{H2O2}$ and the first-order decay rate coefficient k$'_{loss,H2O2}$ (h^{-1}) are the same in the spiked

and unspiked samples:

$$\frac{d\,[H_2O_2]}{dt} = P'_{H2O2} - k'_{loss,H2O2}\,[H_2O_2] \qquad (4)$$

The solution for this differential equation is:

$$[H_2O_2] = \frac{P'_{H2O2}}{k'_{loss,H2O2}}$$
$$- \left\{ \left(\frac{P'_{H2O2}}{k'_{loss,H2O2}} - [H_2O_2]_0 \right) e^{-k'_{loss,H2O2}\,t} \right\} \qquad (5)$$

Time and concentration data for each pair of samples (one unspiked, one spiked with up to 1 mM H$_2$O$_2$) were fitted to equation 5 using the Microsoft Excel solver function. Fitting parameters were global P$'_{H2O2}$ and k$'_{loss,H2O2}$ values, and [H$_2$O$_2$]$_0$ for each sample. For most organisms, three or more replicate measurements (i.e., using three, or more, pairs of spiked/unspiked samples) were performed on each bacterial culture.

Cell-normalized production rates, P$_{H2O2}$, were then calculated with units of amol cell^{-1} hr^{-1} by dividing P$'_{H2O2}$ by the estimated cell count in each syringe (calculated by multiplying cell density in cell mL^{-1} by the volume in mL). Normalized decay rate coefficients k$_{H2O2,cell}$, with units of hr^{-1} (cell mL^{-1}), were calculated by dividing k$'_{loss,H2O2}$ by cell density. The difference in normalization stems from the assumptions that are made about production and decay: namely, that production is proportional to the number of cells present, while the rate of [H$_2$O$_2$] loss in mol L^{-1} hr$^{=1}$ is proportional to the cell density, [cells] as in Cooper et al. (1994):

$$\text{rate of } H_2O_2 \text{ loss} = k_{H2O2,cell}\,[H_2O_2]\,[\text{cells}] \qquad (6)$$

Spiked Batch Incubations With Supernatant

5.00 mL aliquots of each bacterial culture were centrifuged as in section "Measurement of H$_2$O$_2$ Production and Decay Rates by Spiked Batch Incubations." Instead of being discarded, the supernatant was loaded into a syringe and diluted to 50 mL. For each bacterial strain, three pairs of syringes were prepared in this fashion and analyzed by the spiked-batch incubation method. Because there were presumably no cells present in the supernatant, the production and decay data are normalized to the number of cells that originally grew in the medium for comparison purposes.

Incubations with cells were conducted in parallel to incubations of supernatant. After the cultures were centrifuged and the supernatant was removed as described in the previous paragraph, the cells were resuspended in assay medium and centrifuged a second time. The supernatant was removed again, and the cells were resuspended in assay medium before being loaded into a second syringe. The purpose of this additional washing, which was not performed in the other SBI experiments, was to remove all traces of growth medium from the cells.

Conversion Between Rec$_{H2O2}$ and k$'_{loss,H2O2}$

In order to compare H$_2$O$_2$ decay in spiked batch incubations to that in the flow-through method, decay rate coefficients (k$'_{loss,H2O2}$) were converted into recoveries (Rec$_{H2O2}$) and vice versa by assuming that the dead volume in the filter (V, in L) was a well-mixed reactor at steady state (details in Supplementary Material of Schneider et al., 2016). This leads to the equation:

$$k'_{loss,H2O2} = \left(\frac{Q}{V} \right) \left\{ \frac{1}{Rec_{H2O2}} - 1 \right\} \qquad (7)$$

which can also be rearranged to give:

$$Rec_{H2O2} = \frac{\left(\frac{Q}{V} \right)}{k'_{loss,H2O2} + \frac{Q}{V}} \qquad (8)$$

Calculation of Detection Limit for H$_2$O$_2$ Production

The detection limit for P$'_{H2O2}$ in spiked batch incubations can be estimated by realizing that as steady state is approached, the exponential term of equation 5 approaches zero. Thus the steady state concentration of H$_2$O$_2$ is:

$$[H_2O_2]_{ss} = \frac{P'_{H2O2}}{k'_{loss,H2O2}} \qquad (9)$$

Early data in a spiked batch incubation experiment are most important for determining k$'_{loss,H2O2}$, but data collected later, as [H$_2$O$_2$] approaches this steady-state value, are needed to adequately constrain the value of P$'_{H2O2}$. Eq. 9 can therefore be used to estimate the detection limit for P$'_{H2O2}$, DL$_{prod}$, in the spiked batch incubation method:

$$DL_{prod} = DL_{[H2O2]}k'_{loss,H2O2} \qquad (10)$$

where DL$_{[H2O2]}$ is the detection limit for [H$_2$O$_2$]. Thus, the detection limit for P$'_{H2O2}$ is a function of k$'_{loss,H2O2}$ for each species. Dividing by cell density then provides a cell-normalized detection limit of production.

Replicate measurements of [H$_2$O$_2$] at moderate concentrations ($\sim$30 nM) can be made with a typical standard deviation of less than 1 nM; however, near the detection limit of the acridinium ester method, [H$_2$O$_2$] can be determined, at best, with a standard deviation of about 3 nM. We therefore estimate DL$_{[H2O2]}$ as 10 nM for spiked batch incubations.

Estimation of DL$_{prod}$ for the flow-through method was obtained via sensitivity analysis. For each organism, we took a representative data set and adjusted [H$_2$O$_2$]$_{unspiked,cells}$ by 3 nM while holding values for [H$_2$O$_2$]$_{unspiked,direct}$, [H$_2$O$_2$]$_{spiked,cells}$, and [H$_2$O$_2$]$_{spiked,direct}$ constant. The change in P$_{H2O2,cell}$ from the original value was set as DL$_{prod}$ for that organism.

For both of these methods, detection limits were estimated rather than directly measured. As a result, we still report the numerical value of measurement less than an order of magnitude below these detection limits. Such measurements should be assumed to have a high associated uncertainty. We ascribed

any measurement more than an order of magnitude below the detection limit to methodological noise, and report those measurements as zero.

Replicates and Measurement Uncertainties

Statistical significance for all results was assessed using a two-tailed t-test with the minimum level for significance at $p = 0.05$. Reported uncertainties in figures and text represent one standard deviation.

RESULTS AND DISCUSSION

H₂O₂ Decay and Recovery Rates

The eight bacterial strains studied by the flow-through method exhibited a wide range of recovery percentages, ranging from $9 \pm 6\%$ (*Vibrio* sp. A535) to $107 \pm 5\%$ (*Marinobacter* sp. AzsJAc-4) (**Table 2** and **Figure 1**). Conversions yielded decay rate coefficients ranging from $4.0 \pm 0.6 \times 10^{-8}$ hr^{-1} (*Sulfitobacter* sp. EE-36) to $5.2 \pm 2.9 \times 10^{-6}$ hr^{-1} (*Vibrio* sp. A535) (**Table 2**). A decay rate coefficient could not be calculated for *Marinobacter* sp. AzsJAC-4 because of its recovery percentage greater than 100% (**Table 2**).

Decay rate coefficients determined by spiked batch incubations ranged from $2.2 \pm 0.2 \times 10^{-8}$ hr^{-1} (cell mL^{-1})$^{-1}$ for *Tenacibaculum* sp. UAzPsLept-5 to $2.0 \pm 0.1 \times 10^{-6}$ hr^{-1} (cell mL^{-1})$^{-1}$ for *Vibrio* sp. A535. Decay rate coefficients were converted into recovery percentages for comparison purposes and method validation. For each culture evaluated by both flow-through and spiked incubation, there was good agreement between recovery values (two-tailed t-test, $p > 0.05$) for five of the eight organisms, with the exceptions being *Halomonas* sp. VMMm1-3c, *Marinobacter* sp. AzsJAC-4 and *S. oneidensis* sp. MR-1 (**Table 2** and **Figure 1**).

Only one previous study to our knowledge quantified $k_{H2O2,cell}$ for bacterial cultures: Cooper et al. (1994) found $k_{H2O2,cell}$ to be 1.4×10^{-7} hr^{-1} (cells mL^{-1})$^{-1}$ for *Vibrio alginolyticus* and 3.1×10^{-7} hr^{-1} (cells mL^{-1})$^{-1}$ for *E. cloacae*. A value for $k_{H2O2,cell}$ can be inferred for *V. pelagius* in Petasne and Zika (1997) by finding the half-life of H₂O₂ in their Figure 5; this gives a value of 9×10^{-8} hr^{-1} (cells mL^{-1})$^{-1}$. Although these figures are an order of magnitude lower than the $k_{H2O2,cell}$ for *Vibrio* sp. A535, which was found here to be $2.05 \pm 0.22 \times 10^{-6}$ hr^{-1} (cells mL^{-1})$^{-1}$, they are the same order of magnitude as $k_{H2O2,cell}$ for several of the bacterial species in this study.

Decay rate coefficients for the strains studied varied by up to two orders of magnitude. Since decay has previously been linked to cell-surface processes (Moffett and Zafiriou, 1990), we examined the idea that larger decay rates were linked to larger cell surface area. We normalized raw decay rate coefficients (k'_{H2O2}) by total cell surface area and compared these to the previously calculated cell density-normalized decay rate coefficients. The surface-normalized decay rate coefficients also showed a variation of approximately two orders of magnitude

(**Supplementary Figure S1**). Thus, there must be a factor other than cell-surface processes that affect H₂O₂ decomposition.

We also performed spiked batch incubations of supernatant from two bacterial strains (*R. pomeroyi* sp. DSS-3 and *Paracoccus* sp. HIJAc-3c). The raw (non-normalized) decay rate constants for these experiments were 1.2 ± 0.2 hr^{-1} for *R. pomeroyi* sp. DSS-3 and 1.9 ± 0.3 hr^{-1} for *Paracoccus* sp. HIJAc-3c. For both strains, H₂O₂ incubations of the supernatant showed decay that was of a similar magnitude as that of the corresponding cells (**Figure 2A**). These supernatant experiments also indicate that decay may occur by at least two pathways – one (or more) pathways involving cell-surface or intracellular mechanisms, and one (or more) pathways involving secreted soluble enzymes or small molecules. However, we cannot rule out that components originally present in the growth medium contributed to the decay measured in supernatant. It should be emphasized that compounds present in supernatant could not have contributed to measurements in which cells were present (data shown in **Figure 1, Table 2,** and **green** bars in **Figure 2**), since these were conducted on cells resuspended in assay medium. Additionally, cell incubations used as comparisons for the supernatant experiments were rinsed to remove all traces of assay medium; these showed decay rates similar to incubations with unrinsed cells. Control experiments with only artificial seawater showed decay rate coefficients of 0 ± 0 hr^{-1}.

Observations of natural water samples corroborate our suggestion that H₂O₂ decay may be linked to both cell-surface processes and extracellular enzymatic activity, are corroborated by. Previous studies have shown that filtering greatly reduces, but does not completely eliminate, decomposition of H₂O₂. For example, Cooper et al. (1994) showed an increase in half-life from 19.1 h for 1 μm-filtered lake water to 58.1 h for 0.2 μm-filtered lake water, while Yuan and Shiller (2001) observed a decay-rate constant for 0.2 μm-filtered seawater that was half that of unfiltered water. H₂O₂ decay has therefore been strongly linked to microorganisms in natural waters. However, both studies, as well as a subsequent study (Roe et al., 2016) showed non-zero decay rate constants in filtered water. Observations of H₂O₂ decay in ultra-filtered water led Yuan and Shiller (2001) to attribute some decay in unfiltered seawater to colloidal particles. By contrast, autoclaving completely stopped all H₂O₂ decay in coastal seawater (Petasne and Zika, 1997). Since autoclaving would destroy enzymatic activity, this finding, along with the results of the supernatant incubations in the current study, suggests that H₂O₂ decomposition in filtered water is likely dominantly enzymatic.

H₂O₂ Production Rates

For eight of the bacterial strains studied, H₂O₂ production rates were determined by two methods, flow-through and spiked batch incubation, while the remaining four strains were examined only by spiked batch incubation.

Of the eight bacterial strains examined by the flow-through method, four (*Vibrio* sp. A535, *S. oneidensis* sp. MR-1, *Shewanella* sp. ANA-3, and *Halomonas* sp. HIJAc-3c) had all three measurements of P_{H2O2} above the estimated detection limit (blue bars in **Figure 3**), with average P_{H2O2} values of

TABLE 2 | Calculated values for hydrogen peroxide recoveries (Rec$_{H2O2}$) and normalized decay rate coefficient k$_{H2O2,cell}$ for both spiked batch incubation (SBI) and flow-through (FT) methods for SBI.

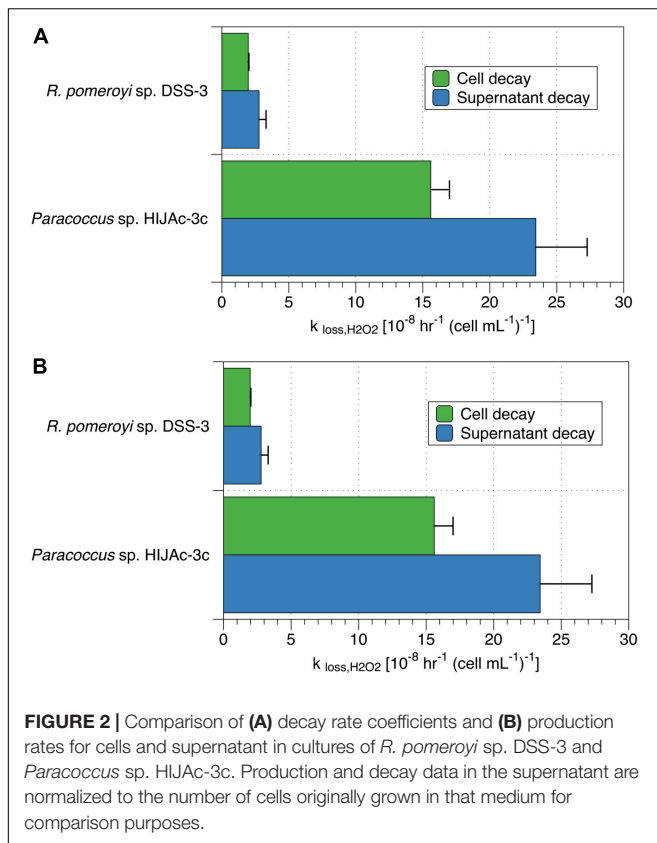| Species	Rec$_{H2O2}$ (%)		k$_{H2O2,cell}$ (10^{-8} hr^{-1} [cell mL^{-1}] $^{-1}$)	
	FT	SBI (from decay)	FT (from Rec$_{H2O2}$)	SBI
A. manganoxydans SI85-9A1	–	13 ± 0	–	25.1 ± 0.1
Bacillus sp. AzsLept-1c	–	63 ± 53	–	102 ± 3
Erythrobacter sp. SD-21	–	11 ± 1	–	31.3 ± 4.5
Halomonas sp. VMMm1-3c	47 ± 5	29 ± 1*	10.4 ± 1.9	5.9 ± 0.2
Marinobacter sp. AzsJAc-4	107 ± 5	6 ± 1*	§	21.1 ± 2.5
Paracoccus sp. HIJAc-3c	40 ± 13	38 ± 3	28.8 ± 13.2	17.7 ± 3.0
R. pomeroyi DSS-3	27 ± 2	23 ± 2	10.9 ± 1.2	6.6 ± 0.7
Shewanella sp. ANA-3	32 ± 15	25 ± 4	5.6 ± 3.0	3.7 ± 0.9
S. oneidensis MR-1	16 ± 4	9 ± 1*	37.0 ± 12.5	10.7 ± 1.5
Sulfitobacter sp. EE-36	35 ± 3	40 ± 9	4.0 ± 0.6	3.5 ± 2.8
Tenacibaculum sp. UAzPsLept-5	–	30 ± 2	–	2.2 ± 0.2
Vibrio sp. A535	9 ± 6	9 ± 1	515 ± 294	205 ± 22

Uncertainties represent one standard deviation. Asterisks represent SBI values of Rec$_{H2O2}$ significantly different from the flow-through values for Rec$_{H2O2}$. §indicates a decay that cannot be calculated due to recoveries over 100%.

FIGURE 1 | Recovery percentages for bacterial strains evaluated with both spiked batch incubations (green bars) and flow-through method (blue bars). Uncertainties represent the standard deviation.

307 ± 207, 2.38 ± 1.40, 0.88 ± 0.53, and 0.78 ± 0.15 amol cell^{-1} hr^{-1}, respectively. Although all measurements were above the detection limit, variation between individual production measurements was great enough that only *Halomonas* sp. VMM1-3c had an average production rate that was significantly different from zero (one-tailed *t*-test, $p > 0.05$). Of the remaining four bacterial strains evaluated, only *Sulfitobacter* sp. EE-36 had any measurements above the detection limit.

Individual measurements of H$_2$O$_2$ production above our estimated detection limit were also observed in the spiked batch incubations, though less consistently than for the flow-through measurements (green bars in **Figure 3**). Of the twelve bacterial strains evaluated, only *Sulfitobacter* sp. EE-36 had all individual production rate measurements over the

detection limit. This strain also had an average value for P$_{H2O2}$ (0.75 ± 0.37) that was significantly different from zero. Seven species (*Halomonas* sp. VMMm1-3c, *Marinobacter* sp. AzsJAc-4, *Paracoccus* sp. HIJAc-3c, *R. pomeroyi* sp. DSS-3, *S. oneidensis* sp. MR-1, *Sulfitobacter* sp. EE-36, and *Tenacibaculum* sp. UAzPsLept-5) met the relatively low criterion of having half or more of their individual production measurements above the detection limit. For these species, average values for P$_{H2O2}$ were 0.59 ± 0.54, 4.67 ± 4.85, 1.05 ± 1.37, 0.15 ± 0.16, 0.34 ± 0.30, 0.75 ± 0.37, and 0.10 ± 0.14 amol cell^{-1} hr^{-1}, respectively. Of the remaining five bacterial strains, three (*Vibrio* sp. A535, *Bacillus* sp. AzsLept-1c, and *Erythrobacter* sp. SD-21) had no measurements over the detection limit, while the remaining two strains (*A. manganoxydans* sp. SI85-9A1 and *Shewanella*

FIGURE 2 | Comparison of **(A)** decay rate coefficients and **(B)** production rates for cells and supernatant in cultures of *R. pomeroyi* sp. DSS-3 and *Paracoccus* sp. HIJAc-3c. Production and decay data in the supernatant are normalized to the number of cells originally grown in that medium for comparison purposes.

sp. ANA-3) had fewer than half of the measurements over the detection limit.

Measurements of P$_{H2O2}$ for supernatant were also obtained and compared to those of cells taken from the supernatant during the incubations described in the previous section (**Figure 2**). In the two bacterial culture supernatants thus evaluated, raw (non-normalized) production rates ranged between 0 and 13 nM hr^{-1} for *R. pomeroyi* sp. DSS-3 and 0 and 31 nM hr^{-1} for *Paracoccus* sp. HIJAc-3c; control experiments in artificial seawater exhibited production rates between 0 and 0.3 nM hr^{-1}. When normalized to the number of cells originally grown in the cultures, *Paracoccus* sp. HIJAc-3c and *R. pomeroyi* sp. DSS-3, P$_{H2O2}$ measurements for growth medium were of a similar magnitude to those of the cells (**Figure 2B**). Production of H$_2$O$_2$ in supernatant could be attributed to enzymes or other exuded labile, redox-active compounds (LRACs) (Zinser, 2018b).

As discussed for decay above, components originally present in the growth medium could have contributed to the production rates measured in the two supernatant experiments. Morris and Zinser (2013) showed that H$_2$O$_2$ production could occur by exposing zwitterionic buffers such as those used in growth media to light. However, the bacteria used in this experiment were grown in a dark incubator, and syringes used for spiked batch incubations were covered between time points. Given the limited light exposure, it is unlikely that H$_2$O$_2$ production in the supernatant is due to light-buffer interactions. Furthermore, the growth medium in question was K medium (Andersen et al., 2005)
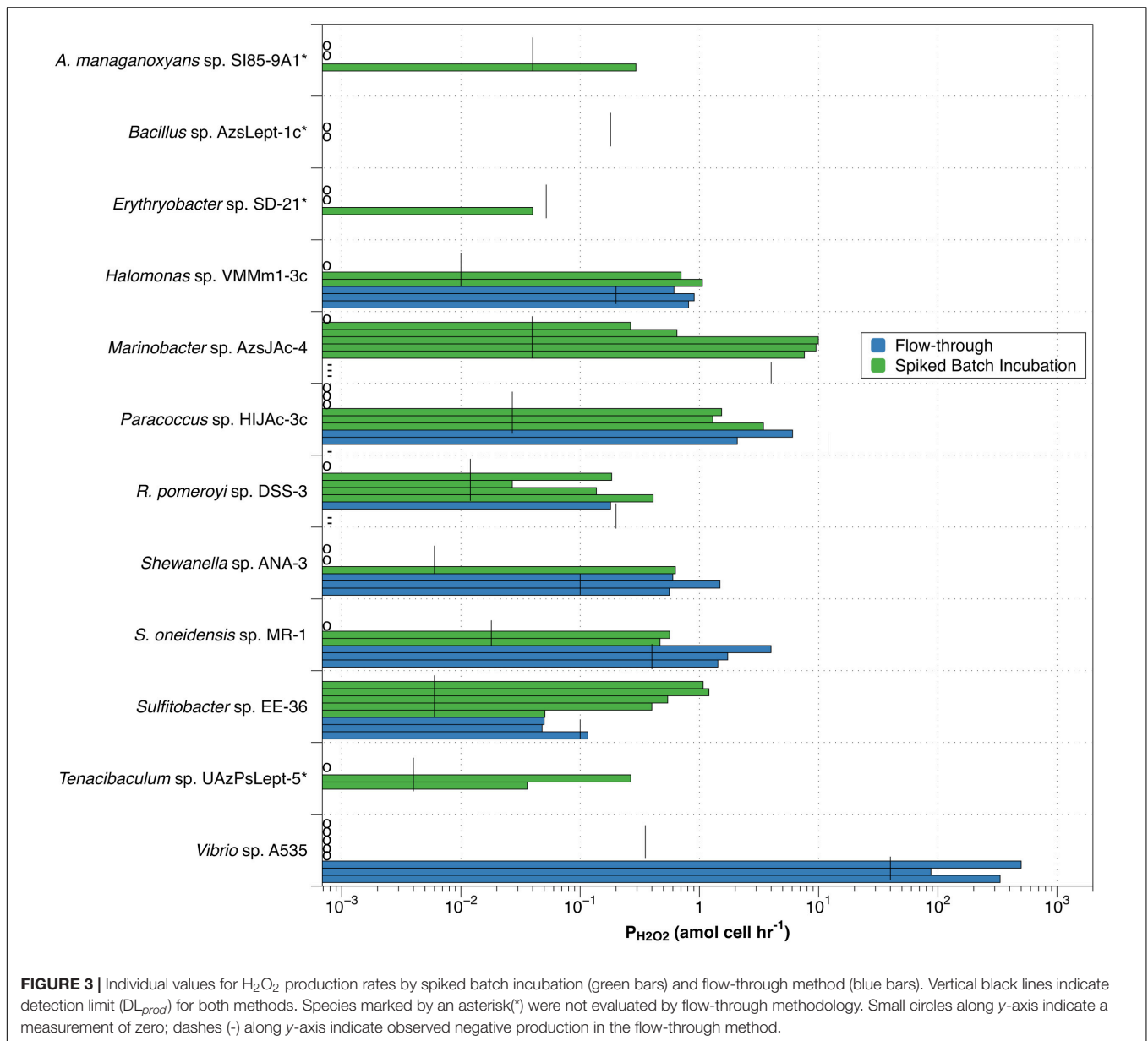
which contains Tris buffer; Morris and Zinser (2013) found that Tris buffer produced considerably less H$_2$O$_2$ than buffers such as HEPES. While we cannot rule out that other compounds in the growth medium contributed to dark H$_2$O$_2$ production measured in supernatant (blue bars in **Figure 2**), they could not have contributed to the production rates measured in the presence of cells (green bars in **Figure 2** and all other measurements presented in this work.) We conclude that observed measurable production in both bacterial cultures and supernatant suggest that both LRACs and cell processes, either inside the cell or on its surface, contribute to P$_{H2O2}$.

Measurement Variability and Comparison Between Spiked Batch Incubation and Flow-Through Methods

Both methods for measuring P$_{H2O2}$ demonstrate high variability. A natural question to ask is whether the fluctuations are due to method limitations or whether the measurements reflect real differences in the behavior of the organisms, for example due to changes in extracellular conditions.

High variability would be expected when measurements were taken close to the calculated detection limit. This would especially be true for the flow-through method, where six of the eight species examined had P$_{H2O2}$ measurements less than an order of magnitude above the detection limit. Spiked batch incubations had lower detection limits, with eight of the strains showing some measurements more than an order of magnitude above detection limit. Yet the variability in P$_{H2O2}$ measurements was higher overall in spiked batch incubations – the standard deviation of the P$_{H2O2}$ measurements was greater than the average P$_{H2O2}$ measurement for 8 out of 12 strains in spiked batch incubations, as opposed to 2 out of 5 for flow-through. Thus, the variability is not clearly linked to measuring P$_{H2O2}$ close to the detection limit.

The observation that, for many of the organisms examined, spiked batch incubation measurements were either well below the detection limit (measurements indicated by a circle along the *y*-axis in **Figure 3**) or well above suggests the possibility that bacteria exist in two states: one in which they produce H$_2$O$_2$ and one in which they do not. This observation applies to eight of the twelve species assessed by spiked-batch incubation – *A. manganoxydans* sp. SI85-9A1, *Halomonas* sp. VMMm1-3c, *Marinobacter* sp. AzsJAc-4, *Paracoccus* sp. HIJAc-3c, *R. pomeroyi* sp. DSS-3, *Shewanella* sp. ANA-3, *S. oneidensis* sp. MR-1, and *Tenacibaculum* sp. UAzPsLept-5. For *Halomonas* sp. VMMm1-3c, *Paracoccus* sp. HIJAc-3c, *R. pomeroyi* sp. DSS-3 and *Shewanella* sp. ANA-3, the ranges of non-zero P$_{H2O2}$ values measured by SBI overlaps with the ranges measured by the flow-through method. This overlap could indicate that the range of non-zero P$_{H2O2}$ measured by either method indicates the strain's H$_2$O$_2$ production while in the "on" mode. However, both for *R. pomeroyi* sp. DSS-3 and for *Paracoccus* sp. HIJAc-3c, the flow-through measurements of P$_{H2O2}$ were below our estimated detection limit for that technique, and also included negative P$_{H2O2}$ measurements (discussed more below), and therefore should be interpreted with caution. It is unclear why replicates grown from the same freezer stocks and, in most cases, sampled

FIGURE 3 | Individual values for H₂O₂ production rates by spiked batch incubation (green bars) and flow-through method (blue bars). Vertical black lines indicate detection limit (DL$_{prod}$) for both methods. Species marked by an asterisk(*) were not evaluated by flow-through methodology. Small circles along y-axis indicate a measurement of zero; dashes (-) along y-axis indicate observed negative production in the flow-through method.

from the same liquid culture would inconsistently "turn on" hydrogen peroxide production. It appears that subtle differences in the environment and handling of the cells can affect the production rate of hydrogen peroxide.

For one bacterial strain, the increased flow rates of the flow-through method may be the "switch" that turns on H₂O₂ production. *Vibrio* sp. A535 had P$_{H2O2}$ values of zero for all of the spiked-batch incubations but, for flow-through measurements, had the highest observed P$_{H2O2}$ values observed in this study. *S. oneidensis* sp. MR-1 showed a less extreme version of this behavior, with H₂O₂ production almost an order of magnitude higher in flow-through than in spiked-batch incubations.

An increase in H₂O₂ production with increasing flow rates has been observed in previous studies of marine algae. We observed that the flow rate used to load diatoms on a filter affected H₂O₂

production by *T. weissflogii* (Schneider et al., 2016). The stress induced by loading cells on the filter by syringe (approximate flow rate 5 mL min^{-1}) induced measured values of P$_{H2O2,cell}$ of 800 amol cell^{-1} hr^{-1}, while cells loaded onto a filter by peristaltic pump (flow rate 0.6 mL min^{-1}) had P$_{H2O2}$ indistinguishable from zero. By contrast, *T. oceanica* had similar values of P$_{H2O2}$ under both conditions. In another study, Shaked and Armoza-Zvuloni (2013) observed a higher release of H₂O₂ from coral with faster stirring. While they attributed this to increased transport of H₂O₂ from the coral to surrounding waters, high stirring speed could also have caused an increase in microbial production of H₂O₂, for example by the microbes in the external mucous layer of the coral. In any case, it is plausible that, analogously to our previous findings for diatoms, higher flow rates cause increased ROS production in some bacterial strains but not in others.

Spiked batch incubations would be expected to have lower values of P$_{H2O2}$ than the flow-through method for those organisms in which flow-related stress affect ROS production.

In contrast, one organism, *Sulfitobacter* sp. EE-36 seems to have lower P$_{H2O2}$ values in flow-through than in spiked batch incubation. What could explain this? As mentioned in section "H$_2$O$_2$ Production Rates," some organisms are likely to produce at least part of their H$_2$O$_2$ by exuding enzymes into their environment. In the two strains whose exudates we studied – *R. pomeroyi* sp. DSS-3 and *Paracoccus* sp. HIJAc-3c – the cell-surface processes seemed about equal to those produced by exuded enzymes. However, different bacterial strains may produce different proportions of their H$_2$O$_2$ via exuded enzymes. In the flow-through method, these enzymes would be continuously washed away by the assay medium; thus, the effect flow has on P$_{H2O2}$ may depend considerably from species to species. Unfortunately, due to time constraints, we were unable to examine supernatant for all bacterial strains and can therefore only speculate exactly how different strains might respond to flow conditions.

Three species, *Paracoccus* sp. HIJAc-3c, *R. pomeroyi* sp. DSS-3 and *Marinobacter* sp. AzsJAc-4, had negative measurements of H$_2$O$_2$ production by the flow-through method (**Supplementary Table S1** and **Supplementary Figure S2**). For two of these, *Paracoccus* sp. HIJAc-3c, *R. pomeroyi* sp. DSS-3, the negative values were small and only appeared in some replicates, and could be accounted for by method uncertainty. However, in the case of *Marinobacter* sp. AzsJAc-4, the negative production rates were consistent and substantial. Since flow-through results accounted for decay and should never yield production rates below zero, this result implies that at least one of our assumptions was not true – most likely, the assumption that decay was first-order with respect to H$_2$O$_2$. If production was low or non-existent, and if the decay rate was less than proportional to [H$_2$O$_2$] (e.g., Michaelis-Menten kinetics), we would expect to see a much smaller drop between [H$_2$O$_2$]$_{spiked,direct}$ and [H$_2$O$_2$]$_{spiked,cells}$ than between [H$_2$O$_2$]$_{unspiked,direct}$ and [H$_2$O$_2$]$_{unspiked,cells}$. In fact, this is what was observed in the case of *Marinobacter* sp. AzsJAc-4 (**Supplementary Figure S3**).

H$_2$O$_2$ Production Compared to O$_2^-$ Production

Since dismutation of O$_2^-$ produces H$_2$O$_2$ in a 2:1 ratio, comparing P$_{H2O2,cell}$ with superoxide production (P$_{O2-,cell}$) allows an evaluation of O$_2^-$ dismutation as a possible production pathway for H$_2$O$_2$. Given high expected variability, average values for P$_{H2O2}$ are not necessarily the best way to express what may be occurring with a particular organism. We have therefore chosen to represent P$_{H2O2}$ graphically as a range of production rates, and compare this to the range of values for P$_{O2-,cell}$ determined by Diaz et al. (2013) (**Figure 4**).

Of the twelve species studied, nine (*A. manganoxydans* sp. SI85-9A1, *Erythrobacter* sp. SD-21, *Halomonas* sp. VMM1-3c, *Marinobacter* sp. AzsJAC-4, *Paracoccus* sp. HIJAc-3c, *R. pomeroyi* sp. DSS-3, *Shewanella* sp. ANA-3, *Sulfitobacter* sp. EE-36, and *Tenacibaculum* sp. UAzPsLept-5; black font in **Figure 4**) have a
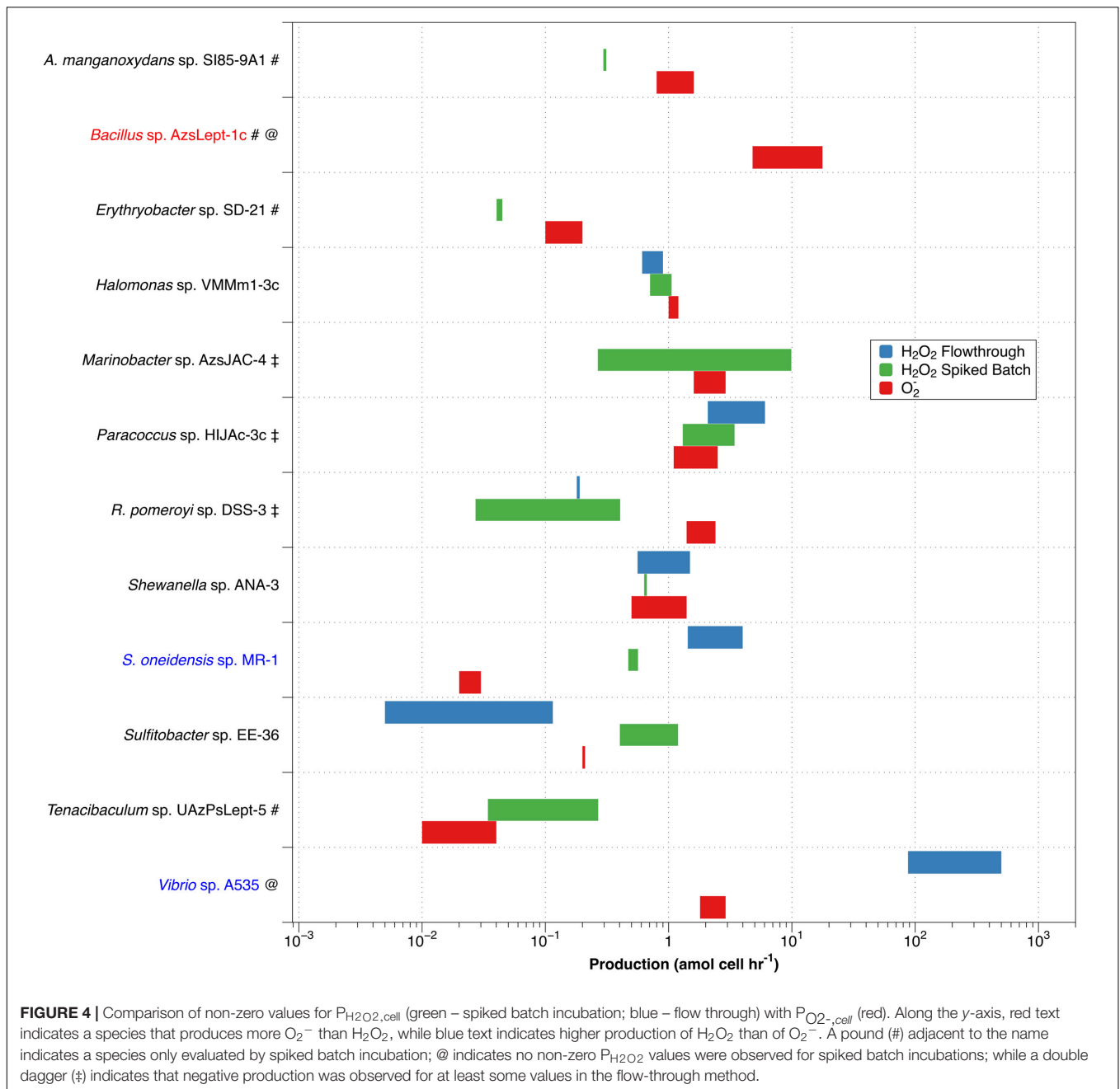
range of P$_{H2O2,cell}$ of comparable magnitude as P$_{O2-,cell}$ (that is, the ranges differ by less than an order of magnitude). Here, P$_{H2O2,cell}$ is not inconsistent with a 2:1 P$_{O2-,cell}$:P$_{H2O2,cell}$ ratio, although a more specific comparison is not available due to the high levels of variability in the measurements. *Bacillus* sp. AzsLept-1c has measurable production of O$_2^-$ but a P$_{H2O2,cell}$ value that is below detection; thus, it produces considerably more O$_2^-$ than H$_2$O$_2$. In this species, small amounts of H$_2$O$_2$ might be produced through the O$_2^-$ dismutation pathway, but O$_2^-$ may also be lost to processes other than dismutation. *S. oneidensis* sp. MR-1 had a range of measured P$_{H2O2,cell}$ values that were substantially higher than P$_{O2-,cell}$. While conflicting results between the flow-through and spiked batch incubation methods make a comparison for *Vibrio* sp. A535 difficult, the flow-through value for P$_{H2O2,cell}$ (which represents conditions closer to those under which the P$_{O2-,cell}$ measurements were made) is two orders of magnitude higher than P$_{O2-,cell}$. Thus, for *Vibrio* sp. A535 and *S. oneidensis* sp. MR-1, it is possible that H$_2$O$_2$ is produced, at least in part, via biological pathways that do not involve O$_2^-$ production.

The variety in P$_{O2-,cell}$:P$_{H2O2,cell}$ ratios is similar to that observed in diatoms of genus *Thalassiosira* (Schneider et al., 2016) and in field studies of freshwater and brackish ponds (Zhang et al., 2016b). In the former study, *T. oceanica* was found to have the 2:1 P$_{O2-,cell}$:P$_{H2O2,cell}$ ratio indicative of production of H$_2$O$_2$ through dismutation, *T. pseudonana* produced considerably more H$_2$O$_2$ than O$_2^-$, and *T. weissflogii* produced considerably less H$_2$O$_2$ than O$_2^-$. Organisms producing more H$_2$O$_2$ than O$_2^-$ have been observed in other studies; for example, *H. carterae* was shown to produce H$_2$O$_2$ but not O$_2^-$ (Palenik et al., 1987). Likewise, Zhang et al. (2016b) observed decoupling of O$_2^-$ and H$_2$O$_2$ production rates in samples taken from freshwater and brackish ponds, with samples showing P$_{O2-,cell}$:P$_{H2O2,cell}$ ratios both below and above the 2:1 ratio that would indicate O$_2^-$ undergoing dismutation to H$_2$O$_2$.

As mentioned previously, the flow rate used to load diatoms on the filter affected H$_2$O$_2$ production by *T. weissflogii* (Schneider et al., 2016). However, we have not previously observed changes in extracellular superoxide production as a function of flow rate, suggesting a decoupling of this response, perhaps because the increased H$_2$O$_2$ is due to intracellular release. For methodological reasons, P$_{H2O2,cell}$ and P$_{O2-,cell}$ were evaluated at different flow rates – 0.6 mL min^{-1} for H$_2$O$_2$ and 2.0 mL min^{-1} for O$_2^-$. This may add to uncertainty in the P$_{O2-,cell}$:P$_{H2O2,cell}$ ratio in flow-through numbers.

Application of Findings to Natural Water Systems

Bacterially mediated decay of H$_2$O$_2$ in natural water systems was estimated by assuming a total bacterial abundance of 10^6 cells mL^{-1} in coastal waters and freshwater and 10^5 cells mL^{-1} in the oligotrophic ocean using the decay rate from *R. pomeroyi* sp. DSS-3 as a typical (near median) decay rate found in this study. The estimated bacterial H$_2$O$_2$ decay rate coefficient in the oligotrophic ocean is 0.007 hr^{-1}, which is considerable in comparison to observed overall values of 0.003 to 0.011 hr^{-1} in

FIGURE 4 | Comparison of non-zero values for $P_{H2O2,cell}$ (green – spiked batch incubation; blue – flow through) with $P_{O2-,cell}$ (red). Along the y-axis, red text indicates a species that produces more O_2^- than H_2O_2, while blue text indicates higher production of H_2O_2 than of O_2^-. A pound (#) adjacent to the name indicates a species only evaluated by spiked batch incubation; @ indicates no non-zero P_{H2O2} values were observed for spiked batch incubations; while a double dagger (‡) indicates that negative production was observed for at least some values in the flow-through method.

the oligotrophic ocean (Petasne and Zika, 1997; Yuan and Shiller, 2001, 2005; AveryJr., Cooper et al., 2005).

In coastal marine and freshwater systems, bacteria also may make a substantial contribution to H_2O_2 decay. Estimated bacterial decay rate coefficients would be approximately 0.066 hr^{-1} which would comprise a substantial fraction of the 0.006 to 0.28 hr^{-1} decay rate coefficient measured in coastal waters (Vermilyea et al., 2010b and references cited therein) or the 0.32 to 0.09 hr^{-1} decay rate coefficients calculated from measured H_2O_2 half-lives in estuarine Chesapeake Bay (Cooper et al., 1994). Freshwaters, which exhibit a wider range of decay rates—observed decay rate coefficients range between

0.11–8.9 hr^{-1} (Cooper et al., 1994; Dixon et al., 2013; Marsico et al., 2015)—could potentially have high bacterial contributions to decay, but more likely it comprises a small percentage of the total. The latter finding corresponds with the findings of Marsico et al. (2015) that dark production in freshwater is most strongly correlated with algal cell counts, with only a weaker correlation to bacterial cell densities.

When assessing the importance of bacteria to regulation of H_2O_2 in natural waters, it is important to consider the wider context of the effects of H_2O_2 on a microbial community. Reactive oxygen species are likely used by a variety of organisms in natural water systems for purposes

such as signaling, allelopathy, and growth (Oda et al., 1995; Diaz and Plummer, 2018). At the same time, high H$_2$O$_2$ levels have been shown to have deleterious effects on aquatic microbial communities, including reduced growth in some bacterial populations (Weinbauer and Suttle, 1999; Morris et al., 2011). This has been attributed to adverse effects on glucose incorporation and respiration processes in bacteria (Santos et al., 2012) caused by the impact of H$_2$O$_2$ on extracellular enzymatic activity (Baltar et al., 2013). Thus, it is necessary for aquatic microbial communities to maintain balanced exogenous H$_2$O$_2$ levels – low enough that important community members are not damaged but high enough that they can function.

However, the burden of decomposing H$_2$O$_2$ is not borne equally by all community members, as shown both previously and within this study. Four of the bacterial strains (*Bacillus* sp. AzsLept-1c, *Halomonas* sp. VMM1-3c, *Marinobacter* sp. AzsJAC-4, and *Tenacibaculum* sp. UAzPsLept-5) within this particular study were isolated from benthic sediments in the same estuary (Elkhorn Slough), yet show decay rate coefficients that vary by up to two orders of magnitude (**Table 2**). Planktonic marine bacteria (e.g., *R. pomeroyi* sp. DSS-3 and *Vibrio* sp. A535) also show a similar range of decay rates. These results correlate with what has been found in previous studies: the cyanobacterium *Prochlorococcus* (Morris et al., 2011) and some strains of the similar bacterium *Synechococcus* (Zinser, 2018a) are completely dependent upon other microbes to scavenge H$_2$O$_2$. If known helper bacterial strains, such as *Alteromonas*, were examined in future studies, we can speculate that they would fall at the higher end of the range of decay rates. However, given that the ability of a particular species to degrade H$_2$O$_2$ may not expressed within a particular community (Morris et al., 2016), it is difficult to predict which bacterial strain might contribute most to H$_2$O$_2$ decay. Nonetheless, it is clear that bacteria have the potential to be major players in regulating H$_2$O$_2$ levels in natural water systems.

The same methodology used to estimate bacterial contributions to H$_2$O$_2$ decay can also be used to approximate dark biological production of H$_2$O$_2$ in natural water systems, again using *R. pomeroyi* as a near-median model organism. Given the uncertainties associated with P$_{H2O2}$ measurements and differences of several orders of magnitude in production rates between planktonic marine bacterial species, these should be considered as order-of-magnitude approximations only. We compare these estimated production rates to studies in which gross (rather than net) values of P$_{H2O2}$ were determined, since the cell-normalized production rates in this study are also calculated by accounting for effects of decay on gross production rates.

Using the median value for P$_{H2O2,cell}$ and 10^5 cells mL^{-1}, bacteria might contribute 0.15 nM hr^{-1} to dark production rates of 0.2 to 3.0 nM hr^{-1} (Roe et al., 2016) in the oligotrophic ocean. Coastal waters would have an estimated bacterial contribution of 1.5 nM hr^{-1}, a substantial fraction of observed gross production rates of 0.8–4.0 nM hr^{-1} (Moffett and Zafiriou,

1990; Vermilyea et al., 2010b). However, the similar rate of 1.5 nM hr^{-1} might be only a tiny fraction of the observed gross dark P$_{H2O2}$ in freshwater, 20–200 nM hr^{-1} in non-oligotrophic freshwaters (Vermilyea et al., 2010b; Marsico et al., 2015). Again, this corresponds with the findings of Marsico et al. (2015) which show no correlation between bacterial abundance and P$_{H2O2}$.

Future Work

While the current study advances the existing understanding of bacterial effects of H$_2$O$_2$ dynamics in natural water systems, in many ways it creates more questions than it answers. First, it reinforces what previous studies have indicated: namely, that H$_2$O$_2$ and O$_2^-$ are created through multiple pathways that may not be coupled to each other. These pathways may be associated with cell-surface processes or with labile redox-active compounds (LRACs) released into the environment. Additional research is needed to determine which processes might be responsible for bacterial production of H$_2$O$_2$ in the strains studied. In particular, further studies of supernatant may help elucidate not only which strains produce LRACs, but also what substances might be catalyzing H$_2$O$_2$ production and decay. With a better understanding of these pathways, genomics and metatranscriptomics might be used to more easily identify which additional strains might be major contributors to H$_2$O$_2$ production in natural water systems.

DATA AVAILABILITY STATEMENT

All datasets generated for this study are included in the article/**Supplementary Material**.

AUTHOR CONTRIBUTIONS

RB, CH, and BV conceived and planned the experiments, and contributed to interpretation of the results. RB carried out the experiments and took the lead in writing the manuscript. BV supervised the project. All authors provided critical feedback and helped to shape the research, analysis, and manuscript.

FUNDING

SUPPLEMENTARY MATERIAL

The Supplementary Material for this article can be found online at: https://www.frontiersin.org/articles/10.3389/fmars.2020.00072/full#supplementary-material

REFERENCES

Andersen, R. A. ed. (2005). *Algal Culturing Techniques*. Amsterdam: Elsevier.

Avery, G. B. Jr., Cooper, W. J., Kieber, R. J., and Willey, J. D. (2005). Hydrogen peroxide at the Bermuda Atlantic Time Series Station: temporal variability of seawater hydrogen peroxide. *Mar. Chem.* 97, 236–244. doi: 10.1016/j.marchem.2005.03.006

Baltar, F., Reinthaler, T., Herndl, G. J., and Pinhassi, J. (2013). Major effect of Hydrogen Peroxide on Bacterial Metabolism in the Northeast Atlantic. *PLoS One* 8:e61051. doi: 10.1371/journal.pone.0061051

Cho, K., Kasaoka, T., Ueno, M., Basi, L., Yamasaki, Y., Kim, D., et al. (2017). Haemolytic activity and reactive oxygen species production of four harmful algal bloom species. *Eur. J. Phycol.* 52, 311–319. doi: 10.1080/09670262.2017.1286525

Cooper, W. J., Moegling, J. K., Kieber, R. J., and Kiddle, J. J. (2000). A chemiluminescence method for the analysis of H$_2$O$_2$ in natural waters. *Mar. Chem.* 70, 191–200. doi: 10.1016/s0304-4203(00)00025-6

Cooper, W. J., Shao, C., Lean, D. R. S., Gordon, A. S., and Scully, F. E. Jr. (1994). *Factors Affecting the Distribution of H2O2 in Surface Waters. In Environmental Chemistry of Lakes and Reservoirs*. Washington, DC: American Chemical Society.

Cooper, W. J., Zika, R. G., Petasne, R. G., and Plane, J. M. C. (1988). Photochemical Formation of H2O2 in Natural Waters Exposed to Sunlight. *Environ. Sci. Technol.* 22, 1156–1160. doi: 10.1021/es00175a004

Diaz, J. M., Hansel, C. M., Voelker, B. M., Mendes, C. M., Andeer, P. F., and Zhang, T. (2013). Widespread Production of Extracellular Superoxide by Heterotrophic Bacteria. *Science* 340, 1223–1226. doi: 10.1126/science.1237331

Diaz, J. M., and Plummer, S. (2018). Production of extracellular reactive oxygen species by phytoplankton: past and future directions. *J. Plankton Res.* 40, 655–666. doi: 10.1093/plankt/fby039

Dixon, T. C., Vermilyea, A. W., Scott, D. T., and Voelker, B. M. (2013). Hydrogen peroxide dynamics in an agricultural headwater stream: evidence of significant nonphotochemical production. *Limnol. Oceanog.* 58, 2133–2144. doi: 10.4319/lo.2013.58.6.2133

Hansel, C. M., Diaz, J. M., and Plummer, S. (2018). Tight Regulation of Extracellular Superoxide Points to Its Vital Role in the Physiology of the Globally Relevant Roseobacter Clade. *mBio* 10: e02668-18. doi: 10.1128/mBio.02668-18

King, D. W., Cooper, W. J., Rusak, S. A., Peake, B. M., Kiddle, J. J., O'Sullivan, D. W., et al. (2007). Flow Injection Analysis of H2O2 in Natural Waters Using Acridinium Ester Chemiluminescence: method Development and Optimization Using a Kinetic Model. *Anal. Chem.* 79, 4169–4176. doi: 10.1021/ac062228w

Learman, D. R., Voelker, B. M., Vazquez-Rodriguez, A. I., and Hansel, C. M. (2011). Formation of manganese oxides by bacterially generated superoxide. *Nat. Geosci.* 4, 95–98. doi: 10.1038/ngeo1055

Marshall, J.-A., Hovenden, M., Oda, T., and Hallegraeff, G. M. (2002). SHORT COMMUNICATION Photosynthesis does influence superoxide production in the ichthyotoxic alga Chattonella marina (Raphidophyceae). *J. Plankton Res.* 24, 1231–1236. doi: 10.1093/plankt/24.11.1231

Marsico, R. M., Schneider, R. J., Voelker, B. M., Zhang, T., Hansel, C. M., and Ushijima, S. (2015). Spatial and temporal variability of widespread dark production and decay of hydrogen peroxide in freshwater. *Aquat. Sci.* 77, 523–533. doi: 10.1007/s00027-015-0399-2

Milne, A., Davey, M. S., Worsfold, P. J., Achterberg, E. P., and Taylor, A. R. (2009). Real-time detection of reactive oxygen species generation by marine phytoplankton using flow injection–chemiluminescence. *Limnol. Oceanogr. Meth.* 7, 706–715. doi: 10.4319/lom.2009.7.706

Moffett, J. W., and Zafiriou, O. C. (1990). An investigation of hydrogen peroxide chemistry in surface waters of Vineyard Sound with H218O2 and 18O2. *Limnol. Oceanog.* 35, 1221–1229. doi: 10.4319/lo.1990.35.6.1221

Morris, J. J., Johnson, Z. I., Szul, M. J., Keller, M., and Zinser, E. R. (2011). Dependence of the Cyanobacterium Prochlorococcus on Hydrogen Peroxide Scavenging Microbes for Growth at the Ocean's Surface. *PLoS One* 6:e16805. doi: 10.1371/journal.pone.0016805

Morris, J. J., Johnson, Z. I., Wilhelm, S. W., and Zinser, E. R. (2016). Diel regulation of hydrogen peroxide defenses by open ocean microbial communities. *J. Plankton Res.* 38:fbw016. doi: 10.1093/fbw016

Morris, J. J., and Zinser, E. R. (2013). Continuous Hydrogen Peroxide Production by Organic Buffers in Phytoplankton Culture Media. *J. Phycol.* 49, 1223–1228. doi: 10.1111/jpy.12123

Oda, T., Moritomi, J., Kawano, I., Hamaguchi, S., Ishimatsu, A., and Muramatsu, T. (1995). Catalase- and superoxide dismutase-induced morphological changes and growth inhibition in the red tide phytoplankton *Chattonella marina*. *Biosci. Biotech. Biochem.* 59, 2044–2048. doi: 10.1271/bbb.59.2044

Palenik, B., Zafiriou, O. C., and Morel, F. M. M. (1987). Hydrogen peroxide production by a marine phytoplankter. *Limnol. Oceanog.* 32, 1365–1369.

Petasne, R. G., and Zika, R. G. (1997). Hydrogen peroxide lifetimes in south Florida coastal and offshore waters. *Mar. Chem.* 56, 215–225. doi: 10.1016/s0304-4203(96)00072-2

Roe, K. L., Schneider, R. J., Hansel, C. M., and Voelker, B. M. (2016). Measurement of dark, particle-generated superoxide and hydrogen peroxide in the subtropical and temperate North Pacific Ocean. *Deep Sea Res. I* 107, 59–69. doi: 10.1016/j.dsr.2015.10.012

Santos, A. L., Gomes, N. C. M., Henriques, I., Almeida, A., Correia, A., and Cunha, A. (2012). Contribution of reactive oxygen species to UV-B-induced damage in bacteria. *J. Photochem. Photobiol.* 117, 40–46. doi: 10.1016/j.jphotobiol.2012.08.016

Schneider, R. J., Roe, K. L., Hansel, C. M., and Voelker, B. M. (2016). Species-level variability in extracellular production rates of reactive oxygen species by diatoms. *Front. Chem.* 4:5. doi: 10.3389/fchem.2016.00005

Shaked, Y., and Armoza-Zvuloni, R. (2013). Dynamics of hydrogen peroxide in a coral reef: sources and sinks. *J. Geo. Res. Biogeo.* 118, 1793–1801. doi: 10.1002/2013JG002483

Shaked, Y., Harris, R., and Klein-Kedem, N. (2010). Hydrogen Peroxide Photocycling in the Gulf of Aqaba. *Red. Sea. Environ. Sci. Technol.* 44, 3238–3244. doi: 10.1021/es902343y

Sutherland, K. M., Coe, A., Gast, R. J., Plummer, S., Suffridge, C. P., Diaz, J. M., et al. (2019). Extracellular superoxide production by key microbes in the global ocean. *Limnol. Oceanog.* 9999, 1–15. doi: 10.1002/lno.11247

van Waasbergen, L. G., Hoch, J. A., and Tebo, B. M. (1993). Genetic analysis of the marine manganese-oxidizing *Bacillus* sp. *Strain SG*-1: protoplast transformation, Tn917 mutagenesis, and identification of chromosomal loci involved in manganese oxidation. *J. Bacteriol.* 175, 7594–7603. doi: 10.1128/jb.175.23.7594-7603.1993

Vermilyea, A. W., Dixon, T. C., and Voelker, B. M. (2010a). Use of H218O2 to Measure Absolute Rates of Dark H2O2 Production in Freshwater Systems. *Environ. Sci. Technol.* 44, 3066–3072. doi: 10.1021/es100209h

Vermilyea, A. W., Hansard, S. P., and Voelker, B. M. (2010b). Dark production of hydrogen peroxide in the Gulf of Alaska. *Limnol. Oceanog.* 55, 580–588. doi: 10.4319/lo.2010.55.2.0580

Waring, J., Klenell, M., Bechtold, U., Underwood, G. J. C., and Baker, N. R. (2010). Light-induced responses of oxygen photoreduction, reactive oxygen species production and scavenging in two diatom species. *J. Phycol.* 46, 1206–1217. doi: 10.1111/j.1529-8817.2010.00919.x

Weinbauer, M. G., and Suttle, C. A. (1999). Lysogeny and prophage induction in coastal and offshore bacterial communities. *Aquat. Microb. Ecol.* 18, 217–225. doi: 10.3354/ame018217

Yuan, J., and Shiller, A. M. (2001). The distribution of hydrogen peroxide in the southern and central Atlantic ocean. *Deep Sea Res. II* 48, 2947–2970. doi: 10.1016/s0967-0645(01)00026-1

Yuan, J., and Shiller, A. M. (2005). Distribution of hydrogen peroxide in the northwest Pacific Ocean. *Geochem. Geophys. Geosys* 6:Q09M02

Zhang, T., Diaz, J. M., Brighi, C., Parsons, R. J., McNally, S., Apprill, A., et al. (2016a). Dark Production of Extracellular Superoxide by the Coral *Porites astreoides* and Representative Symbionts. *Front. Mar. Sci.* 3:232. doi: 10.3389/fmars.2016.00232

Zhang, T., Hansel, C. M., Voelker, B. M., and Lamborg, C. H. (2016b). Extensive Dark Biological Production of Reactive Oxygen Species in Brackish and Freshwater Ponds. *Environ. Sci. Technol.* 50, 2983–2993. doi: 10.1021/acs.est.5b03906

Zinser, E. R. (2018a). Cross-protection from hydrogen peroxide by helper microbes: the impacts on the cyanobacterium *Prochlorococcus* and other beneficiaries in marine communities. *Environ. Microbiol. Rep.* 10, 300–411. doi: 10.1111/1758-2229.12625

Zinser, E. R. (2018b). The microbial contribution to reactive oxygen species dynamics in marine ecosystems. *Environ. Microbiol. Rep.* 10, 412–427. doi: 10.1111/1758-2229.12626